Liegt aus

Internal Report
DESY D3-84
June 1996

Doses due to neutrons and charged particles in the angular range 10° to 170° behind concrete shield of high energy proton accelerators

H. Dinter, K. Tesch
Deutsches Elektronen-Synchrotron DESY, Hamburg, Germany

and
D. Dworak
Institute of Nuclear Physics, Krakow, Poland

Internal Report
DESY D3-84
June 1996

Doses due to neutrons and charged particles in the angular range 10° to 170° behind concrete shield of high energy proton accelerators

H. Dinter, K. Tesch
Deutsches Elektronen-Synchrotron DESY, Hamburg, Germany
Notkestr. 85, 22603 Hamburg, Germany

and
D. Dworak
Institute of Nuclear Physics, Krakow, Poland
ul. Radzikowskiego 152, 31–342 Krakow, Poland

To be published

Abstract

Spectra and dose equivalents of neutrons, protons, and pions behind ordinary concrete shields or iron-loaded concrete shields are calculated. The results are parametrized by means of a simple formula.

1. Introduction

The neutron field behind the side shielding of proton accelerators with primary energies above a few GeV is well known. Many measurements and calculations were published in the last years. Some of our more recent results can be found in [1]-[3]. The side shield is the most important geometry in practice, and simple formulae are available (see, e.g., [2]) to calculate the maximum neutron dose for a beam incident on a thick target. Photon doses behind shieldings are calculated in [4].

What is missing are neutron doses $H_n(\theta)$ and dose attenuation coefficients $\lambda_H(\theta)$ in the total angular range and the contribution of charged particles to the total dose. A systematic study of these subjects are not available at present. We calculated these quantities for a spherical shield around an extended target. Such a geometry allows a clear definition of dose values and attenuation coefficients as a function of the angle θ against the direction of the incoming proton beam (in contrast to the side shielding geometry). Spherical shields are not realized in practice, but magnitudes like $H_n(30°)$ and the corresponding attenuation behaviour may be useful for practical cases. And the knowledge of the dose of charged particles is important for selecting dose measuring systems.

2. The source

The Monte-Carlo program FLUKA in its version 92 [5] was used for all calculations together with a data library from ENEA [6].

First we studied the production of secondary radiation from an iron target with a small diameter (1 cm ø · 60 cm long) so that the spectra were not much disturbed by thick target material. The energy of the one-dimensional proton beam was 100 GeV. Particle fluences were calculated at a distance of 5 m from the target as a function of the angle θ; the center was the middle of the target. The results are displayed in fig. 1 for neutrons and protons with energies above 150 MeV and between 20 and 150 MeV, for pions of both signs above 20 MeV, and kaons and antiprotons above 50 MeV. It gives the characteristic difference between the steep angular distribution of high energy neutrons, protons, and pions, and the rather flat distribution of cascade neutrons and cascade protons. Kaons and antiprotons can be neglected in the following. The spectra (fig. 2) show the expected contribution of cascade particles around 100 MeV at 90° together with the evaporation neutrons. The angular dependence of the spectra can be characterized by the mean energies of particles above 20 MeV which are given in tab. 1.

The fluence in backward direction is higher than around 90°. This is an effect of the target extended in beam direction, more generations of particles can contribute at large angles near 180°. The particle spectrum is also harder than at 90° since the production of a particle of the third or fourth generation is a forward-production process for the preceding parent generation. This can be shown by calculating the spectrum as a function of generations. A consequence is a dose attenuation coefficient increasing with increasing angles in backward direction, see section 4.

3. Calculation of dose equivalents behind concrete shields

In order to calculate dose equivalents and dose equivalent attenuation coefficients in the angular range 10° to 170° we assumed an iron target 4 cm ø · 60 cm surrounded by a spherical concrete shell with a thickness of 5 m and positioned at distance r between 5 and 10 m from the center of the target. The angular range is divided in 10° or 20° intervals. The steep angular dependence shown in fig. 1 could disturb the attenuation in a given angular interval due to a contribution of particles emitted into the next smaller interval and scattered into the interval under question. Therefore only particles emitted from the target into the angular interval under study were transported; only this interval and the adjacent intervals were filled with concrete (to allow for backscattering), all other regions remained empty. The one-dimensional proton beam was allowed to interact behind the front face of the target. The distance r between 5 and 10 m was divided in intervals of 0.5 m. Particles were scored when they cross these boundaries within the angular interval under study , then their fluence was calculated.

For high energy particles the maximum dose equivalent in a 30-cm phantom must be considered. Calculating the maximum is important for neutrons above 20 MeV, their dose maximum moves from the surface into the phantom with increasing energy. And this is especially important in the case of charged particles when the peak of their Bragg curve falls inside the phantom. Therefore we take the fluence-to-dose conversion factors from ICRP21 [9], Appendix 6 and 7, and from ICRP51 [10], tab. 23 col. 2, tab. 25a col. 2, and tab. 16a. The calculation of the ambient dose equivalent at a depth of 10 mm (see, e.g., [7], [8]) underestimates the detrimental effect of radiation. Therefore the quantity ambient dose equivalent should not be used at high energy accelerators.

4. Results

Most of our results concern neutrons, the main component of the radiation field. It is known that neutron spectra are independent of concrete thicknesses used in practice and are independent of the primary proton energy above a few GeV. An example of their angular dependence is shown in fig. 3a–c. Though it is difficult to achieve good statistical accuracy one recognizes the shaping effect of 2 m concrete (by comparison with fig. 2) and the θ-dependence of the contribution above 150 MeV.

We calculated the neutron dose equivalent per proton, H_n, for primary proton energies E_p = 10, 100 and 1000 GeV, thickness d of ordinary concrete up to 5 m, and θ from 10° to 170°. In all cases the magnitude $H_n r^2$ showed in exponential decrease for all d larger then a d_{min} (r = distance from middle of target to region of interest). For $d < d_{min}$ and at angles below 50° a dose build-up occurs due to the presence of neutrons in the 0.5–5 GeV range; at angles above 50° the dose decreases strongly within d_{min} owing to the absorption of low energy neutrons produced in the target. H_n is a function of r, d, θ, E_p, target dimension and material, and type of concrete. The E_p dependence is known to be of the type E_p^a with a $\approx$ 0.8. We received a = 0.69 in the range 10–1000 GeV. The length of our iron target is 60 cm or about 4 nuclear interaction lengths which is long enough to produce the typical particle spectrum behind a concrete shield. The dependence of H_n on the target diameter was examined in [2]; we assume without prove that the resulting target factor f_T can be used in the present cases. Then our results can be given as

$$H_n = \frac{H_{no}(\theta)}{r^2}\, E_p^{0.69} f_T \; e^{-\frac{d}{\lambda(\theta)}} \; ; \; d > d_{min} \tag{1}$$

The parameters H_{no} $(\theta), \lambda(\theta)$ and d_{min} are given in tab. 2; E_p is in GeV. The strong angular dependence is expected and corresponds to the changing high energy part of the neutron spectrum (cf. figs. 2 and 3). The reason for the slight increase of H_n and λ in backward direction is already mentioned in section 2.

The equation can be compared with the formula for calculating the neutron dose behind a side shield parallel to the proton beam; it is presented, e.g., in [2] together with most recent parameters. Both give nearly the same $H_n\, r^2$ values if an angle $\theta = 70°$ is chosen (the difference is about 35% for d = 1.5 or 3 m; in the side shielding formula r and d are lines perpendicular to the beam). At $\theta = 90°$ the value is smaller. It is known that the dose maximum along a side shield occurs at angles smaller than 90° with respect to the target, and the contribution of neutrons produced at small angles and scattered to regions at around 90° are explicitely excluded in the present calculations.

The same calculations were performed for iron-loaded heavy concrete with a density of 3.7 g/cm^3. Its composition is 50.0% iron, 34.4% oxygen, 6.8% silicon, 6.8% calcium, 1.0% aluminium, 0.4% hydrogen by weight. A neutron spectrum at 90° behind 1.2 m thickness is displayed in fig. 3 d and demonstrates the better shielding property against high energy neutrons. Its shielding parameters for the equation above are also entered into tab. 2. For completeness its parameters for the side shielding formula in [2] are also given here:
$H_o = 9.7 \cdot 10^{-15}$ Sv m^2 and $\lambda' = 140$ g/cm^2.

The dose equivalents of protons and pions behind ordinary concrete were calculated up to about 3 m of concrete. Their spectra were determined up to 2 m and for E_p = 10, 100, and 1000 GeV. In these intervals they were found to be independent of the primary proton energy and of shield thickness and have shapes not very different from those shown in fig. 2. At 10°–20° they extend from 40 to 2000 MeV (1/10 values), the mean energy of protons is 250 MeV and that of pions 350 MeV. At 90° their ranges are 20 to 500 MeV, and their mean energies are 70 MeV and 150 MeV, respectively. The ratios of the dose equivalents of charged particles to that of neutrons is of practical interest, they are shown in fig. 4. The H_p/H_n values could be averaged over the primary energies 10–1000 GeV, they are nearly independent of the shielding thickness. The "cascade protons" are in equilibrium with cascade neutrons above 20 MeV, both are products of the intranuclear cascade. Such an equilibrium does not exist for pions, they are produced mainly in the target and dominate the total dose equivalent at small angles and for high primary energies. The ratios in fig. 4 are for 100 and 1000 GeV primary proton energy, for 10 GeV they are lower. For practical shielding geometries the pion doses can be neglected.

Our charged particle results can be compared with the reports of Roesler and Stevenson [8] and of Gorbatkov and Kryuchkov [11]. The ratio of charged particle fluence $\phi_{p,\pi}$ to the fluence of neutrons with energies above 20 MeV, ϕ_{hn}, is used for comparison in order to avoid the discussion of different fluence-to-dose conversion coefficients; concrete shield thickness is about 1 m, E_p ≈100 GeV, and $\theta \approx 50°$ to 100° (side shield). We find $\phi_p/\phi_{hn} = 0.03$ and $\phi_\pi/\phi_{hn} = 0.014$ in reasonable agreement with [8] giving 0.02 and 0.015, respectively. The agreement is expected since the same Monte Carlo code FLUKA was used. (The dose equivalent of charged particles from [8] are much lower than in the present paper for reasons mentioned in section 3). A completely different approach are the calculations in [11]. Here the program ROZ6H is used which uses a discrete ordinates method for solving the multigroup kinetic equation of particle transport: the multigroup cross sections are from a system called SADCO-2. The side shielding geometry has to be transformed approximately into a one-dimensional model. It is satisfying that essentially one can state agreement regarding neutron spectra above 10 keV and neutron penetration in concrete or iron shield thicknesses of practical importance. In contrast to that, the resulting fluences of protons and pions are much higher. The authors receive ratios ϕ_p/ϕ_{hn} = 0.24 and $\phi_\pi/\phi_{hn} = 0.04$. They quote two experiments the results of which are in favor of these higher values. Apparently a systematic experimental study of charged particle doses behind shielding is necessary.

References

1. H. Dinter and K. Tesch, Radiat.Prot.Dosimetry 42 (1992) 5

2. H. Dinter, K. Tesch and D. Dworak, Nucl.Instr.Meth. A 368 (1996) 265, 273.

3. H. Dinter and K. Tesch, Radiat.Prot.Dosimetry 63 (1996) 175

4. D. Dworak, K. Tesch and J.M. Zazula, Nucl.Instr.Meth. A 321 (1992) 589

5. A. Fassò, A. Ferrari, J. Ranft, P.R. Salla, G.R. Stevenson and J.M. Zazula, Proc. Workshop on Simulating Accelerator Radiation Environment, Santa Fe, 1993

6. E. Cuccoli, A. Ferrari and G.C. Panini, JEF-DOC-340 (1991)

7. A.V. Sannikov and E.N. Savitskaya, CERN TIS/RP/TM/93-38 (1993)

8. S. Roesler and G.R. Stevenson, CERN TIS-RP/IR/93-47 (1993)

9. ICRP Publication 21, Pergamon Press, 1973

10. ICRP Publication 51, Pergamon Press, 1987

11. D.V. Gorbatkov, V.P. Kryuchkov, Protvino, IHEP 95-73 (1995)

Tab. 1. Mean energies of secondary radiation produced by 100-GeV protons on an iron target.

Angular interval	$\bar{E}$(MeV) n	p	$\pi^{\pm}$
0–5°	3000	4000	4500
5–10°	1200	1200	1800
20–30°	230	280	550
80–100°	75	90	180

Tab. 2 Parameters for eq. 1.

Angular interval	Ordinary concrete			Heavy concrete		
	λ (g/cm^2)	H_{no} (Sv m^2)	d_{min} (m)	λ (g/cm^2)	H_{no} (Sv m^2)	d_{min} (m)
10–20°	166	3.3–13	1.3	185	4.1–13	0.6
20–30°	150	1.0–13	0.8	169	1.3–13	0.4
30–40°	139	5.9–14	0.7	159	6.9–14	0.3
40–50°	137	3.3–14	0.2	150	4.5–14	0.2
50–60°	127	2.4–14	0.0	141	3.2–14	0.1
60–70°	123	1.5–14	0.2	136	2.2–14	0.0
70–80°	113	1.1–14	0.5	129	1.4–14	0.2
80–100°	110	6.1–15	0.6	124	7.8–15	0.4
100–120°	103	4.1–15	0.6	123	4.2–15	0.6
120–140°	117	2.1–15	0.8	136	2.5–15	0.7
140–150°	113	3.0–15	0.6	161	1.8–15	1.0
150–160°	130	3.6–15	0.5	161	3.0–15	0.6
160–170°	149	4.2–15	0.4	158	5.5–15	0.1

Figure captions

Fig. 1 Fluence of particles produced by one 100-GeV proton on an iron target as a function of angle against proton beam dirction. The distance is 5 m.

Fig. 2 Spectra of neutrons, protons, and pions produced by 100-GeV protons on an iron target at 2 angular intervalls. Each spectrum is normalized to unity.

Fig. 3 Neutron spectra produced by 100-GeV protons behind concrete shields.
a) - c) : 2 m ordinary concrete 3 angular intervals.
d) 1.2 m heavy concrete. Each spectrum is normalized to unity.

Fig. 4 Ratios of proton dose equivalent or pion dose equivalent to total neutron dose equivalent as a function of angle and concrete shield thickness.

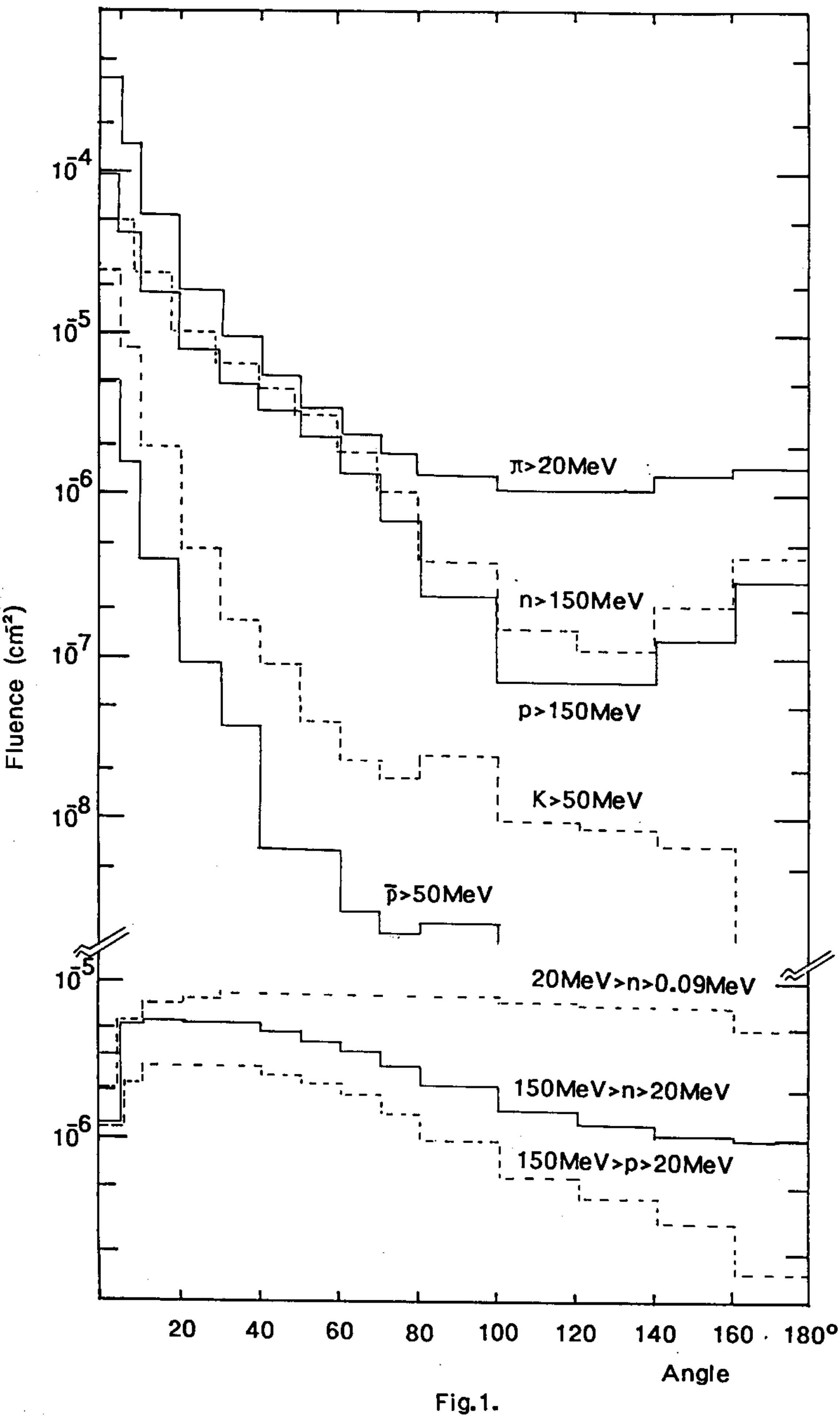

10^{-4}
10^{-5}
10^{-6}
10^{-7}
10^{-8}
10^{-5}
10^{-6}
Fluence (cm^{-2})
π>20MeV
n>150MeV
p>150MeV
K>50MeV
p̄>50MeV
20MeV>n>0.09MeV
150MeV>n>20MeV
150MeV>p>20MeV
20
40
60
80
100
120
140
160
180°
Angle

Fig.1.

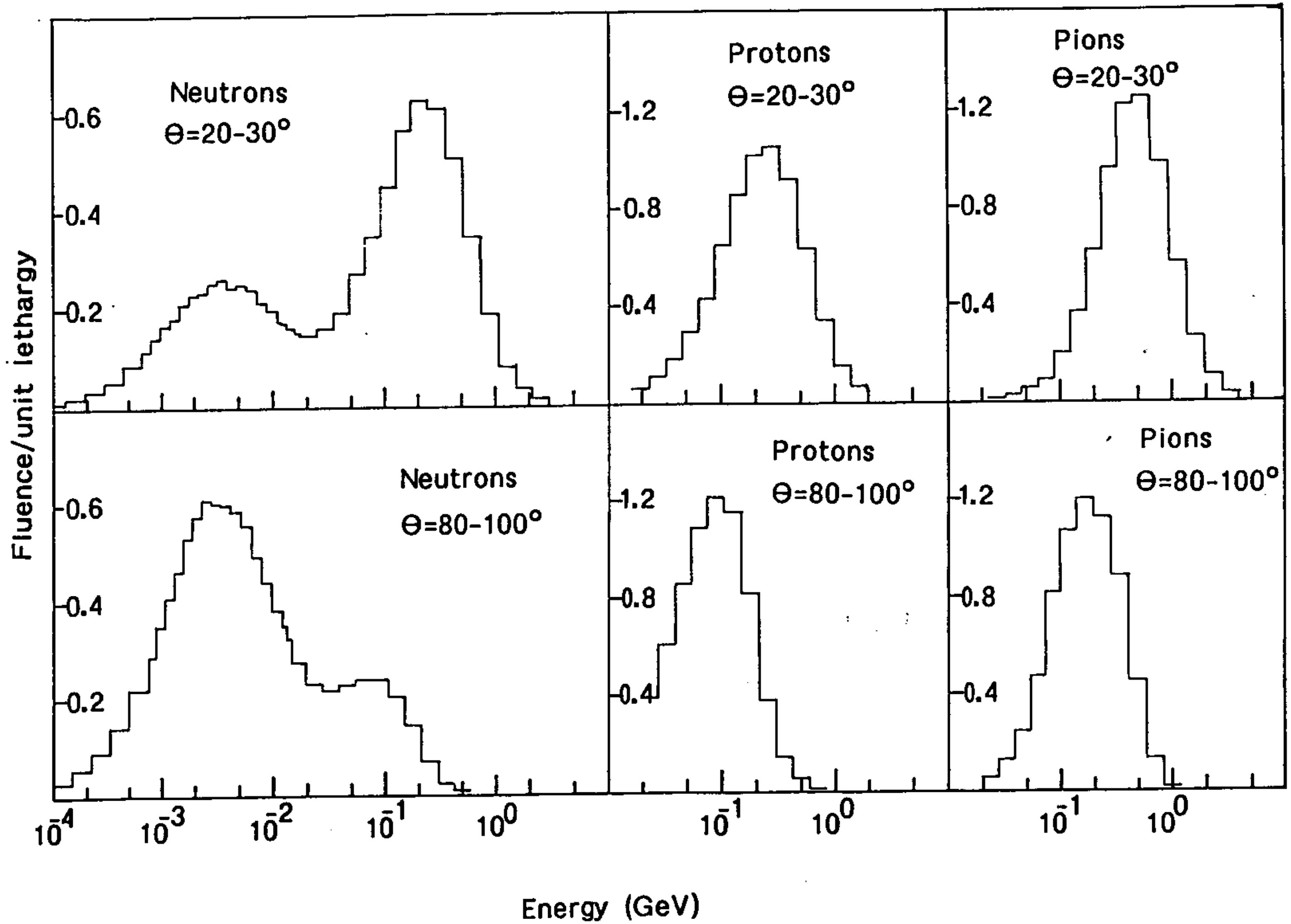

Neutrons
Θ=20-30°
Protons
Θ=20-30°
Pions
Θ=20-30°
Neutrons
Θ=80-100°
Protons
Θ=80-100°
Pions
Θ=80-100°
0.6
0.4
0.2
1.2
0.8
0.4
Fluence/unit lethargy
10⁻⁴
10⁻³
10⁻²
10⁻¹
10⁰
Energy (GeV)

Fig.2.

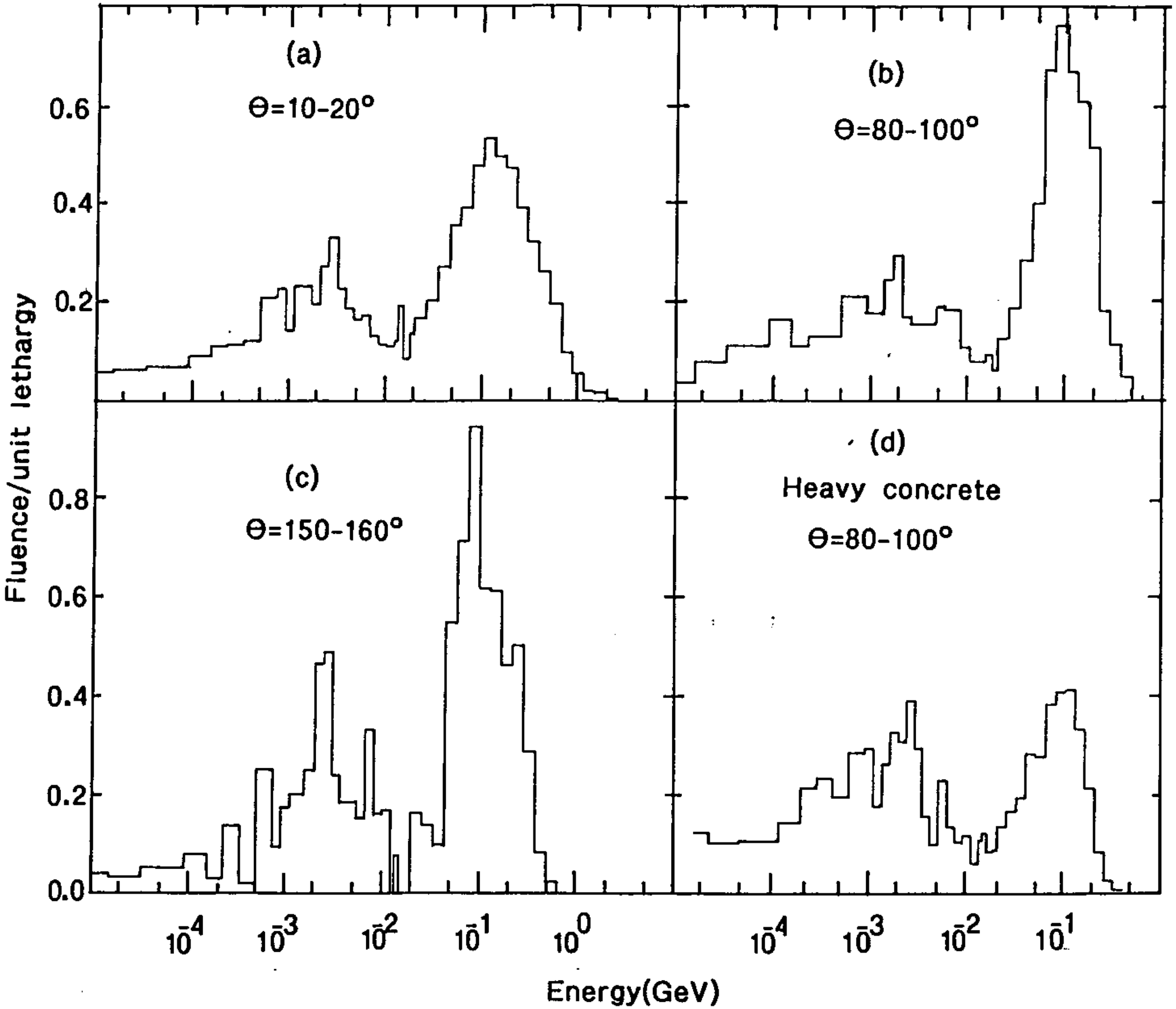
(a)
Θ=10-20°
(b)
Θ=80-100°
(c)
Θ=150-160°
(d)
Heavy concrete
Θ=80-100°
Fluence/unit lethargy
0.6
0.4
0.2
0.8
0.0
10⁻⁴
10⁻³
10⁻²
10⁻¹
10⁰
Energy(GeV)

Fig.3.

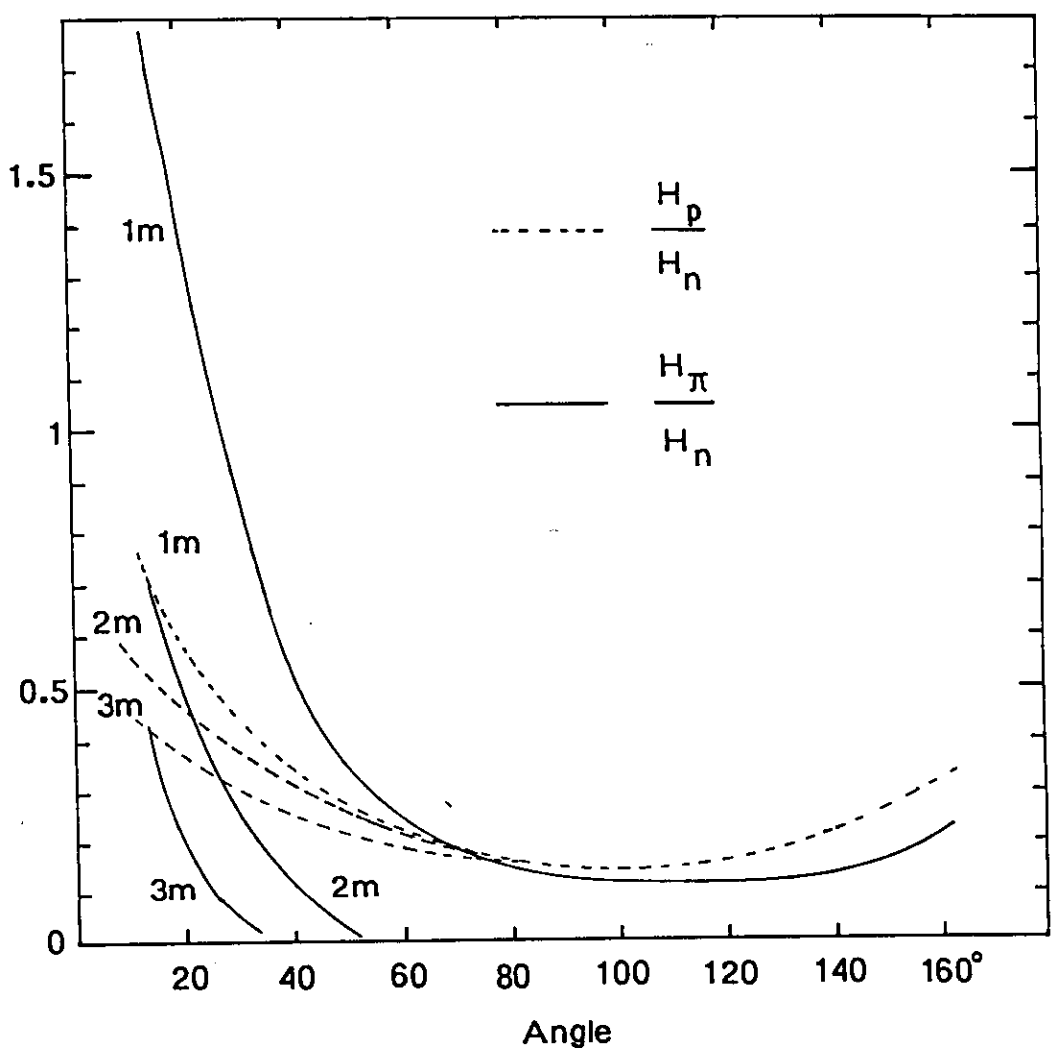

1.5
1
0.5
0
20
40
60
80
100
120
140
160°
Angle
1m
1m
2m
3m
3m
2m
H_p/H_n
H_π/H_n

Fig.4.